IEEE Access
Multidisciplinary ⋮ Rapid Review ⋮ Open Access Journal

Received October 13, 2021, accepted November 2, 2021, date of publication December 10, 2021,
date of current version December 24, 2021.

Digital Object Identifier 10.1109/ACCESS.2021.3134829

Secure Communication Based on Hyperchaotic Underactuated Projective Synchronization

KEVIN HERMAN MURARO GULARTE[1], LUCAS MARTINS ALVES[1], JOSÉ ALFREDO RUIZ VARGAS[1], SADEK CRISÓSTOMO ABSI ALFARO[2], GUILHERME CARIBE DE CARVALHO[2], AND JESUS FRANKLIN ANDRADE ROMERO[3]

[1]Departamento de Engenharia Elétrica, Universidade de Brasília, Brasília, Federal District 70910-900, Brazil
[2]Departamento de Engenharia Mecânica, Universidade de Brasília, Brasília, Federal District 70910-900, Brazil
[3]Centro de Engenharia, Modelagem e Ciências Sociais Aplicadas, Universidade Federal do ABC, Santo André, São Paulo 09210-580, Brazil

Corresponding author: José Alfredo Ruiz Vargas (vargas@unb.br)

This work was supported in part by the Coordenação de Aperfeiçoamento de Pessoal de Nível Superior (CAPES), Brazil, under Finance Code 001.

ABSTRACT This paper proposes a scheme for secure telecommunication based on the projective synchronization of hyperchaotic systems. The design of the synchronizer considers the presence of disturbances to increase the robustness of the method. The main advantage of the proposed approach lies in that only two control inputs are required to synchronize the master and slave systems. Hence, the control structure is simple, which, in turn, simplifies the applications. Based on Lyapunov theory, the proposed approach ensures the finite-time convergence of the synchronization error to a small neighborhood of the origin, even in the presence of disturbances in all states. Simulations to both show the advantages and applications of the proposed approach were also accomplished to validate the theory.

INDEX TERMS Cryptography, hyperchaotic systems, projective synchronization, Lyapunov theory.

I. INTRODUCTION

In the past few years, significant progress has been made in the study of chaotic systems. Chaotic systems are deterministic nonlinear systems that show sensitive dependence on initial conditions and have an aperiodic behavior [1]. A necessary condition for a system to be chaotic lies in that at least one Lyapunov exponent be positive [2]. The chaotic motion on a strange attractor was first discovered in the 60s by Lorenz [3]. In the following years, some relevant chaotic models, such as those by Rössler [4], Chen and Ueta [5], Sprott [6], and Lüand Chen [7], were introduced. More recently, many works have been proposed in the literature. See, for example, [8]–[11].

On the other hand, a system can exhibit hyperchaos when at least two of their associated Lyapunov exponents are positive, and its dimension is higher than three [12]. Hyperchaos was initially introduced in 1979 by Rössler [13]. Since then, other important models have been proposed. Refer to [2], [14]–[26] and the references therein to quote a few.

Chaotic and hyperchaotic systems have been used in most diverse contexts, including nonlinear identification [27]–[29], observation and control [30], [31], economy [32], [33], welding [34], [35], and secure communication [11], [21], [36], [37], [39]–[42]. In particular, chaos-based cryptography is a very active research topic in the literature, which is motivated by the pseudo-random behavior observed in chaotic systems. Typical applications encompass, for example, the generation of pseudo-random numbers for encryption and decryption of messages [43]–[47]. The main technologies used for implementation are analog electronics [21], [24], [48], field-programmable gate array (FPGA) [43], [49], microcontrollers [50], [51], and digital signal processing (DSP) [52]. It should be noted that chaos has a less complex and unpredictable behavior than hyperchaos, as claimed in [53]. Hence, the use of hyperchaos can sometimes be more suitable than chaos for secure communication [54], [55].

Synchronization lies in adjusting the dynamic behavior of two dynamic systems, known as master (drive) and slave (response), so that their trajectories converge in time. The synchronization of chaotic systems was first introduced in 1990 [56]. Several classes of synchronization have been proposed since then: antisynchronization (AS) [57], lag synchronization (LS) [58], projective synchronization (PS) [16], [59]–[63], modified projective synchronization (MPS) [61],

The associate editor coordinating the review of this manuscript and approving it for publication was Wonhee Kim.

and function projective synchronization FPS [64]. In general, the synchronization type depends on a scaling factor. For instance, PS is characterized by a constant proportional synchronization between the master and slave systems. Hence, identical and AS are particular cases of this kind of synchronization with scaling factors 1 or -1. Matrix and functional scaling factors define MPS and FPS, respectively. However, most of the synchronization works above are only valid under either fully-actuated control or matching condition [65].

Also, interesting contributions have been proposed in [11], [17], [19], [20], [23], [26], [60], [66]–[68]. However, in these works, the usage of disturbances in the stability and convergence analysis was not considered.

In summary, the synchronization of either chaos or hyperchaos is characterized by two main hypotheses: the control dimension and system order are equal [9], [17], [19], [20], [39], [61], [63], [66], [69], [70] and unknowns are not considered in the stability analysis [11], [17], [19], [20], [23], [26], [60], [66]–[68]. The former is related to the complexity of the synchronization scheme and the latter to the robustness of the method. Synchronization of underactuated hyperchaotic systems is rarely found in the literature. Also, to the best of our knowledge, the robust projective synchronization of underactuated hyperchaotic systems is not present in the literature. It should be noted that underactuation is a condition defined by a higher number of independent variables than control signals [71]. Thus, underactuated systems have fewer actuators than degrees of freedom [72]–[75], i.e., the control dimension is lesser than the state dimension. The main significance of the underactuated projective synchronization is the reduction of actuators in diverse applications.

Motivated by the previous facts, this work presents a robust scheme for projective synchronization of a hyperchaotic system to overcome the aforementioned drawbacks. Hence the proposed approach is based on both Lyapunov theory (to ensure boundedness and finite-time convergence) and underactuated control law (to simplify the application). More specifically, this paper presents the following contributions.

1) An underactuated projective synchronization scheme for a perturbed Zhou *et al.* hyperchaotic system [20] is proposed. The proposed synchronization has a simple structure, in contrast to [9], [17], [19], [20], [22], [23], [39], [53], [61], [63], [69], [70], [76].

2) Neither matching condition nor fully-actuated control is assumed, i.e., the analysis considers that disturbances are present in all states, even in those without actuation, and all states are not used in the proposed synchronization mechanism. In contrast to [11], [17], [19], [20], [23], [26], [60], [66]–[68].

3) The proposed scheme is applied to secure communication, and it was implemented using electrical circuits. In contrast to [17], [19], [20], [23], [26], [61], [63], [69], [70], [76], [77].

It should be noted that a simple structure leads to easier implementations. The consideration of disturbances in the stability analysis aim at robustness against disturbances which are inevitable in actual applications. To the best of our knowledge, this is the first time that a robust underactuated projective synchronization method for hyperchaotic systems is proposed in the literature.

The work is organized as follows. In Section II, the problem and main assumptions are introduced. The synchronization error is presented in Section III. In Section IV, a control law, which ensures that the synchronization errors are bounded and finite-time convergent, is proposed. Section V is concerned with application of the proposed method in secure telecommunication. In Section VI, the development of an electronic circuit for the implementation of the proposed method is accomplished, and a comparison study with another work in the literature is performed. Finally, the conclusions of the paper are drawn in Section VII.

II. PROBLEM STATEMENT

Consider the following master hyperchaotic system [20]:

$$\begin{cases} \dot{x}_m = a(y_m - x_m) - w_m \\ \dot{y}_m = bx_m - x_m z_m - y_m \\ \dot{z}_m = x_m y_m - cz_m \\ \dot{w}_m = dx_m z_m - kw_m \end{cases} \tag{1}$$

Based on (1), a perturbed slave hyperchaotic system can be defined as

$$\begin{cases} \dot{x}_s = a(y_s - x_s) - w_s + h_1 + u_1 \\ \dot{y}_s = bx_s - x_s z_s - y_s + h_2 \\ \dot{z}_s = x_s y_s - cz_s + h_3 \\ \dot{w}_s = dx_s z_s - kw_s + h_4 + u_4 \end{cases} \tag{2}$$

where x_m, y_m, z_m, and w_m are the state variables of the master system (1); x_s, y_s, z_s, and w_s are the state variables of the slave system (2); h_1, h_2, h_3, and h_4 are the disturbances; u_1 and u_4 are the control signals. The system parameters satisfy $a \in [10, 25]$, $b \in [10, 50]$, $c \in [1, 3]$, $d \in [1, 2]$, and $k \in [-1, 2]$ [20].

The aim of this work lies in the synchronization of (1) and (2) by using an underactuated control scheme, for any initial condition, even in the presence of unmatched disturbances.

Fact 1: With the boundedness of the system (1), the following inequalities are true:

$$\begin{aligned} |x_m(t)| &\leq \bar{x} \\ |y_m(t)| &\leq \bar{y} \\ |z_m(t)| &\leq \bar{z} \\ |w_m(t)| &\leq \bar{w} \end{aligned} \tag{3}$$

$\forall t \geq 0$, where $\bar{x}$, $\bar{y}$, $\bar{z}$, and $\bar{w}$ are unknown positive constants.

Assumption 1: It is assumed that the disturbances in (2) are bounded. More specifically,

$$\begin{aligned} |h_1(t)| &\leq \bar{h}_1 \\ |h_2(t)| &\leq \bar{h}_2 \\ |h_3(t)| &\leq \bar{h}_3 \\ |h_4(t)| &\leq \bar{h}_4 \end{aligned} \tag{4}$$

$\forall t \geq 0$, where $\bar{h}_1$, $\bar{h}_2$, $\bar{h}_3$, and $\bar{h}_4$ are unknown positive constants.

Remark 1: It is noteworthy that systems (1) and (2) are, in general, different, due to the presence of disturbances. Besides, our approach assumes that all these disturbances are not in the control span. Hence, the control signal can not be used straightforwardly to tackle with them. However, we will exploit the master boundedness and the particular structure of (1)-(2), in the next sections, to devise a simple and robust control law.

Remark 2: Note that Equation (1) does not have a disturbance term. That is no loss of generality because any disturbance in (1) would join with those in (2) in the stability analysis.

III. PROJECTIVE SYNCHRONIZATION ERROR

In this section, the main error associated with the synchronization problem is defined.

The projective synchronization error is defined as

$$\begin{aligned} e_1 &= x_s - \delta x_m \\ e_2 &= y_s - \delta y_m \\ e_3 &= z_s - \delta z_m \\ e_4 &= w_s - \delta w_m \end{aligned} \tag{5}$$

where δ is a nonzero constant defined by the user.

Based on (1)-(2), the time-derivative of (5) results

$$\begin{aligned} \dot{e}_1 &= -ae_1 + ae_2 - e_4 + h_1 + u_1 \\ \dot{e}_2 &= -e_2 + be_1 - e_1e_3 - \delta z_m e_1 - \delta x_m e_3 \\ &\quad - (\delta^2 - \delta)x_m z_m + h_2 \\ \dot{e}_3 &= -ce_3 + e_1e_2 + \delta y_m e_1 + \delta x_m e_2 \\ &\quad + (\delta^2 - \delta)x_m y_m + h_3 \\ \dot{e}_4 &= -ke_4 + de_1e_3 + d\delta z_m e_1 + d\delta x_m e_3 \\ &\quad + (\delta^2 - \delta)dx_m z_m + h_4 + u_2 \end{aligned} \tag{6}$$

IV. LYAPUNOV STABILITY ANALYSIS

After the formulation of the synchronization error equations, the next step is selecting a control law. In what follows, we consider a standard Lyapunov function candidate V, which hinges upon the synchronization error, and choose a control law to make $\dot{V}$ lower than zero outside a compact region at the origin Ω. The key drivers for the design are then the peculiar structure of (2), boundedness of (1), and an enlargement process for constraining $\dot{V}$ to be negative definite outside Ω.

Theorem 1: Consider the master and slave systems (1)-(2), Assumption 1, and the control laws

$$\begin{aligned} u_1 &= -\psi_1 e_1 - \psi_2 e_1 e_4^2 \\ u_4 &= -\psi_3 e_4 \end{aligned} \tag{7}$$

If

$$\begin{aligned} \psi_1 &> \delta_1 \\ \psi_2 &> \frac{d^2}{2} \\ \psi_3 &> \delta_2 \end{aligned} \tag{8}$$

Then, the synchronization error is ultimately bounded. It converges in finite-time to the compact set

$$\Omega = \left\{ e \in \Re^4 \mid \|e\| \leq \theta < \xi \right\} \tag{9}$$

where the convergence time holds

$$t_{max} = \begin{cases} 0 & \text{if } e(t) \in \Omega \\ \dfrac{1}{\rho} ln \left[\dfrac{V(0)}{\frac{\xi^2}{2} - \frac{\beta}{\rho}} \right] & \text{otherwise} \end{cases} \tag{10}$$

and $\delta_1 = 0.5[\sigma_1 \bar{h}_1^2 + \sigma_5(a^2 + b^2 + \delta^2 \bar{z}^2) + \sigma_6 \delta^2 \bar{y}^2 + \sigma_7(d\delta\bar{x} + 1)] - a$, $\delta_2 = 0.5\left(\sigma_4 \bar{h}_4^2 + \frac{d\delta\bar{x}+1}{\sigma_7} + \frac{d^2\delta^2\bar{x}^2}{\sigma_8} + \sigma_{11}\right) - k$, $\theta = \sqrt{\frac{2\beta}{\rho}}$, $\xi > 0$, $\beta = \beta_u + \beta_n + \beta_\delta$, $\frac{\rho}{2} = min\{\rho_1, \rho_2, \rho_3, \rho_4\}$, $\beta_u = 0.5\left(\frac{1}{\sigma_1} + \frac{1}{\sigma_4}\right)$, $\beta_n = 0.5\left(\frac{\bar{h}_2^2}{\sigma_2} + \frac{\bar{h}_3^2}{\sigma_3}\right)$, $\beta_\delta = 0.5(\delta^2 - \delta)^2\left(\frac{\bar{x}^2\bar{z}^2}{\sigma_9} + \frac{\bar{x}^2\bar{y}^2}{\sigma_{10}} + \frac{\bar{x}^2\bar{z}^2}{\sigma_{11}}\right)$, $\rho_1 = \psi_1 - \delta_1$, $\rho_2 = 1 - 0.5\left(\sigma_2 + \frac{1}{\sigma_5} + \sigma_9\right)$, $\rho_3 = c - 0.5\left(\sigma_3 + \frac{1}{\sigma_6} + \sigma_8 + \sigma_{10} + 1\right)$, $\rho_4 = \psi_3 - \delta_2$, $\|e\|^2 = e_1^2 + e_2^2 + e_3^2 + e_4^2$, and $\sigma_i, i = 1, \ldots, 11$ are positive constants.

Proof: Consider the following Lyapunov function candidate

$$V = \frac{\|e\|^2}{2} \tag{11}$$

The time-derivative of (11) results

$$\dot{V} = e_1\dot{e}_1 + e_2\dot{e}_2 + e_3\dot{e}_3 + e_4\dot{e}_4 \tag{12}$$

By replacing (6) in (12), we have

$$\begin{aligned} \dot{V} &= e_1(-ae_1 + ae_2 - e_4 + h_1 + u_1) \\ &\quad + e_2[-e_2 + be_1 - e_1e_3 - \delta z_m e_1 - \delta x_m e_3 \\ &\quad - (\delta^2 - \delta)x_m z_m + h_2] \\ &\quad + e_3[-ce_3 + e_1e_2 + \delta y_m e_1 + \delta x_m e_2 \\ &\quad + (\delta^2 - \delta)x_m y_m + h_3] \\ &\quad + e_4[-ke_4 + de_1e_3 + d\delta z_m e_1 + d\delta x_m e_3 \\ &\quad + (\delta^2 - \delta)dx_m z_m + h_4 + u_2] \end{aligned} \tag{13}$$

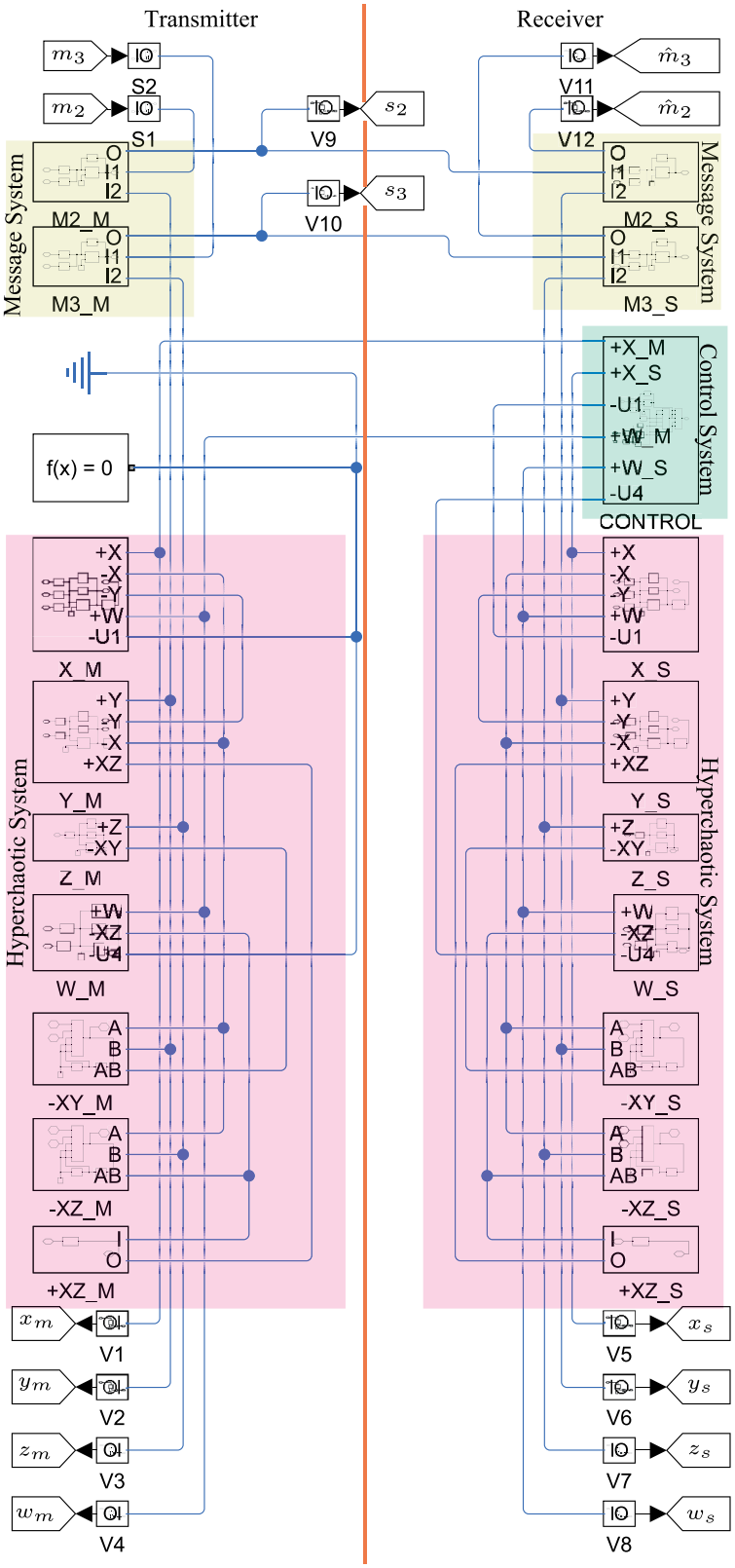

FIGURE 1. Circuit diagram. M2_M, M3_M, M2_S, M3_S are the encryption/ decryption blocks (Figure 5). U1 and U4 are generated by the CONTROL block (Figure 2). X_M and X_S are the *X* state blocks (Figure 6). Y_M and Y_S are the *Y* state blocks (Figure 7). Z_M and Z_S are the *Z* state blocks (Figure 8). W_M and W_S are the *W* state blocks (Figure 9). +XZ_M and +XZ_S are the inversion blocks (Figure 3). −XZ_M, −XZ_S, −XY_M, and −XY_S are the multiplication blocks (Figure 4). V1 to V12 are voltage to signal converters and the S1 and S2 are signal to voltage converters of the Simulink.

Also, by employing (7) in (13), we obtain

$$\begin{aligned}\dot{V} = &-(\psi_1 + a)e_1^2 - e_2^2 - ce_3^2 - (\psi_3 + k)e_4^2 \\ &- \psi_2 e_1^2 e_4^2 + h_1 e_1 + h_2 e_2 + h_3 e_3 + h_4 e_4 + e_1 e_2(a \\ &+ b - \delta z_m) + \delta y_m e_1 e_3 + e_1 e_4(d\delta z_m - 1) \\ &+ d\delta x_m e_3 e_4 - (\delta^2 - \delta) x_m z_m e_2 \\ &+ (\delta^2 - \delta) x_m y_m e_3 + (\delta^2 - \delta) x_m z_m e_4 \\ &+ d e_1 e_3 e_4 \end{aligned} \tag{14}$$

On the other hand, from Fact 1, Assumption 1, and Young's inequality, it follows that

$$\begin{aligned} e_1 h_1 &\leq \frac{\sigma_1 e_1^2 \bar{h}_1^2}{2} + \frac{1}{2\sigma_1}; \quad e_2 h_2 \leq \frac{\sigma_2 e_2^2}{2} + \frac{\bar{h}_2^2}{2\sigma_2} \\ e_3 h_3 &\leq \frac{\sigma_3 e_3^2}{2} + \frac{\bar{h}_3^2}{2\sigma_3}; \quad e_4 h_4 \leq \frac{\sigma_4 e_4^2 \bar{h}_4^2}{2} + \frac{1}{2\sigma_4} \\ & e_1 e_2(a + b - \delta z_m) \\ &\leq \frac{\sigma_5(a^2 + b^2 + \delta^2 \bar{z}^2) e_1^2}{2} + \frac{e_2^2}{2\sigma_5} \\ \delta y_m e_1 e_3 &\leq \frac{\sigma_6 \delta^2 \bar{y}^2 e_1^2}{2} + \frac{e_3^2}{2\sigma_6} \\ e_1 e_4(d\delta x_m - 1) &\leq \frac{\sigma_7 e_1^2 (d\delta \bar{x} + 1)}{2} + \frac{e_4^2 (d\delta \bar{x} + 1)}{2\sigma_7} \\ d\delta x_m e_3 e_4 &\leq \frac{\sigma_8 e_3^2}{2} + \frac{d^2 \delta^2 \bar{x}^2 e_4^2}{2\sigma_8} \\ -(\delta^2 - \delta) x_m z_m e_2 &\leq \frac{\sigma_9 e_2^2}{2} \\ &+ \frac{(\delta^2 - \delta)^2 \bar{x}^2 \bar{z}^2}{2\sigma_9} \\ (\delta^2 - \delta) x_m y_m e_3 &\leq \frac{\sigma_{10} e_3^2}{2} + \frac{(\delta^2 - \delta)^2 \bar{x}^2 \bar{y}^2}{2\sigma_{10}} \\ (\delta^2 - \delta) x_m z_m e_4 &\leq \frac{\sigma_{11} e_4^2}{2} + \frac{(\delta^2 - \delta)^2 \bar{x}^2 \bar{z}^2}{2\sigma_{11}} \\ d e_1 e_3 e_4 &\leq \frac{e_3^2}{2} + \frac{d^2 e_1^2 e_4^2}{2} \end{aligned} \tag{15}$$

Based on (15), (14) implies

$$\begin{aligned}\dot{V} \leq &-e_1^2(\psi_1 - \delta_1) - e_2^2 \rho_2 - e_3^2 \rho_3 - e_4^2(\psi_3 - \delta_2) + \beta_u \\ &+ \beta_n + \beta_\delta - \left(\psi_2 - \frac{d^2}{2}\right) e_1^2 e_4^2 \end{aligned} \tag{16}$$

By using (8), (16) can be written as

$$\dot{V} \leq -\rho V + \beta \tag{17}$$

Then, one can see that $\dot{V} < 0$ in (17) when $e \in \Omega^T$. Since Ω is a compact set, the errors starting inside Ω will remain there forever. In case that the errors start outside Ω, it can be seen that $\dot{V} < 0$, then V and, consequently, $\|e\|$ will decrease monotonically until the errors enter Ω at some finite time t_{max}.

To determine t_{max}, it should be noted that (17) implies ([78], Lemma 3.2.4)

$$V(t) \leq \left[V(0) - \frac{\beta}{\rho}\right] \exp(-\rho t) + \frac{\beta}{\rho} \tag{18}$$

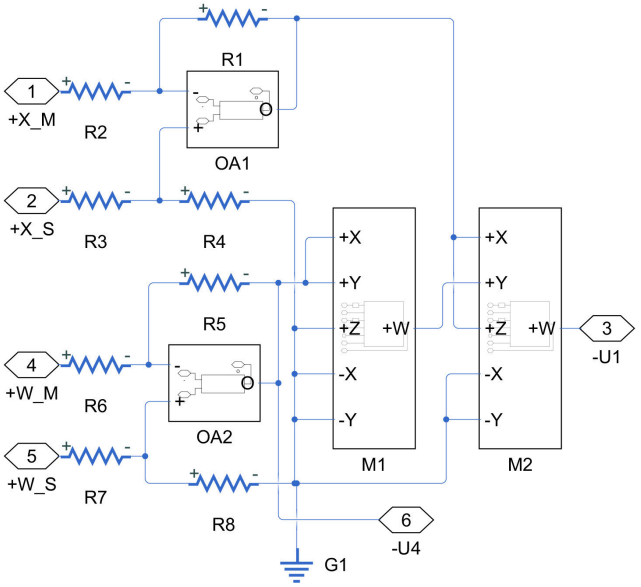

FIGURE 2. CONTROL block circuit. R1 = R4 = R5 = R8 = 100kΩ and R2 = R3 = R6 = R7 = 1kΩ with tolerance of 0.1%. The blocks OA1 and OA2 are operational amplifiers OPA228. The blocks M1 and M2 are analog multipliers AD633JNZ.

which further yields

$$t_{max} = \frac{1}{\rho} ln \left\{ \frac{V(0)}{\frac{\xi^2}{2} - \frac{\beta}{\rho}} \right\} \tag{19}$$

Therefore, (19) shows that the synchronization error converges to the compact set Ω at least in a finite-time t_{max} and, hence ([79]), that the this error is ultimately bounded. □

Remark 3: The main idea of the proposed method lies in the usage of the system structure and Lyapunov theory to design an adequate control law. Based on a trial-and-error procedure, we considered all possibilities of underactuated control in the analysis and the simplest one was chosen. Young's inequality was used in the stability analysis in the process to make $\dot{V} < 0$ outside of a small compact set, whose size can be decreased by increasing the control gains, even in the presence of bounded unmatched disturbances.

Remark 4: Integrator backstepping [80], [81] and sliding mode [26], [82] are also used in the control of underactuated systems. However, most works based on backstepping suffer from "the explosion of complexity," and, in general, the presence of matched disturbances is assumed. See, for example, [80], [81]. On the other hand, sliding mode control suffers from chattering, and the disturbances are also supposed to be matched [81]. Besides, most of synchronizers based on hyperchaotic systems found in the literature employ complete actuation [8], [53], [83], [84]. Then, the main peculiarity of our work, in contrast to the literature, thus lies in that neither matching condition nor fully-actuated control is assumed.

Remark 5: Note that the performance of the proposed method, as far as the residual synchronization error is considered, is affected by the control gains ψ_1 and ψ_3, scaling

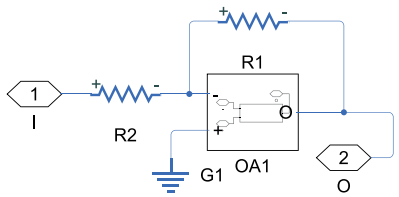

FIGURE 3. Inverter block circuit. R1 = R2 = 10kΩ with tolerance of 0.1%. The block OA1 is an operational amplifier OPA228.

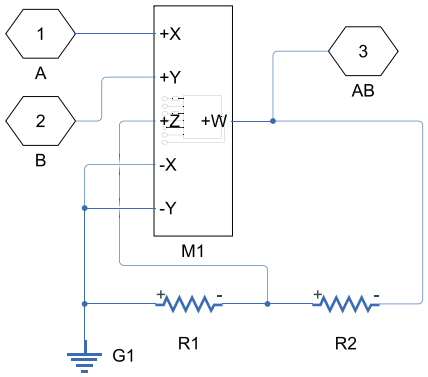

FIGURE 4. Multiplier block circuit. R1 = R2 = 10kΩ with tolerance of 0.1%. The block M1 is an analog multiplier AD633JNZ.

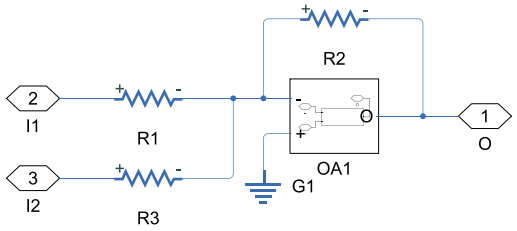

FIGURE 5. Encryption/decryption block circuit. R1 = R2 = R3 = 100kΩ with tolerance of 0.1%. The block OA1 is an operational amplifier OPA228.

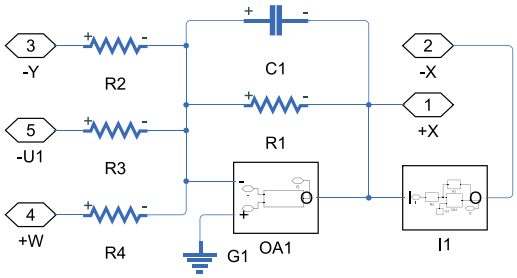

FIGURE 6. State *X* block circuit. C1 = 10nF, R1 = R2 = 10kΩ, and R3 = R4 = 100kΩ. Resistors and capacitors have a tolerance of 0.1%, OA1 is an operational amplifier OPA228 and I1 is an inversion block (Figure 3).

factor δ, disturbances, and upper bounds for the states of the master system, as can be seen from (8) and the definitions below (10). In general, the performance for the actuated states can be arbitrarily enhanced by increasing ψ_1 and ψ_3. For non-actuated states, although there is a complex relationship between β and ρ in (9), the performance can also be indirectly controlled through ψ_1 and ψ_3 since higher control gains can

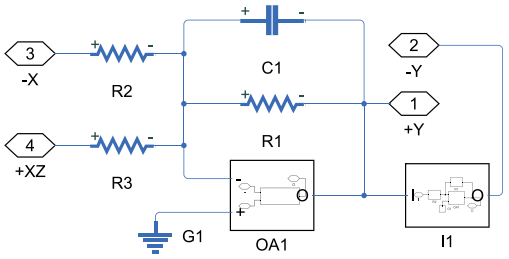

FIGURE 7. State *Y* block circuit. C1 = 10nF, R1 = 100kΩ, R2 = 2.1kΩ, and R3 = 1kΩ. Resistors and capacitors have a tolerance of 0.1%, OA1 is an operational amplifier OPA228 and I1 is an inversion block (Figure 3).

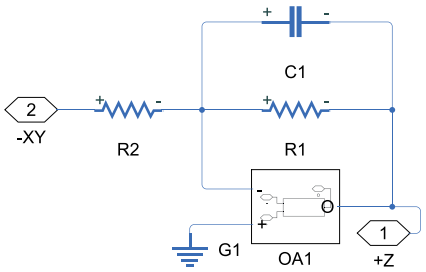

FIGURE 8. State *Z* block circuit. C1 = 10nF, R1 = 100kΩ, and R2 = 1kΩ. Resistors and capacitors have a tolerance of 0.1% and OA1 is an operational amplifier OPA228.

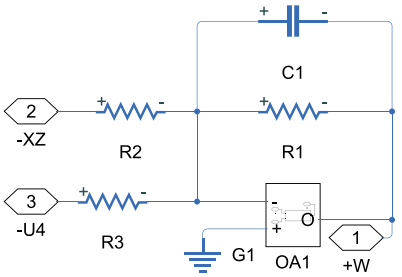

FIGURE 9. State *W* block circuit. C1 = 10nF, R1 = 50kΩ, R2 = 1kΩ, and R3 = 100kΩ. Resistors and capacitors have a tolerance of 0.1% and OA1 is an operational amplifier OPA228.

allow for higher ρ in (9), as can be seen from the stability analysis.

Remark 6 (Selection of the Control Gains): By replacing the parameters in (8) and considering the case of identical synchronization ($\delta = 1$), (8) can be rewritten as

$$\begin{aligned}\psi_1 &> 0.5[\sigma_1\bar{h}_1^2 + \sigma_5(400 + 1024 + \bar{z}^2) + \sigma_6\bar{y}^2 \\ &\quad + \sigma_7(\bar{x} + 1)] - 20 \\ \psi_2 &> 0.5 \\ \psi_3 &> 0.5\left(\sigma_4\bar{h}_4^2 + \frac{\bar{x}+1}{\sigma_7} + \frac{\bar{x}^2}{\sigma_8} + \sigma_{11}\right) + 1 \end{aligned} \tag{20}$$

In addition, one can select conservative values for the bounds and other parameters as $\bar{x} = 27$, $\bar{y} = 38$, $\bar{z} = 63$, $\bar{w} = 240$, $\bar{h}_1 = 2.7$, $\bar{h}_2 = 3.8$, $\bar{h}_3 = 6.3$, $\bar{h}_4 = 24$, $\sigma_1 = 1$, $\sigma_4 = \frac{1}{2}$, $\sigma_5 = 1$, $\sigma_6 = 1$, $\sigma_7 = 1$, $\sigma_8 = 1$, and $\sigma_{11} = \frac{1}{2}$. Then $\psi_1 > 3429.29$ and $\psi_3 > 523.75$. It should be noted

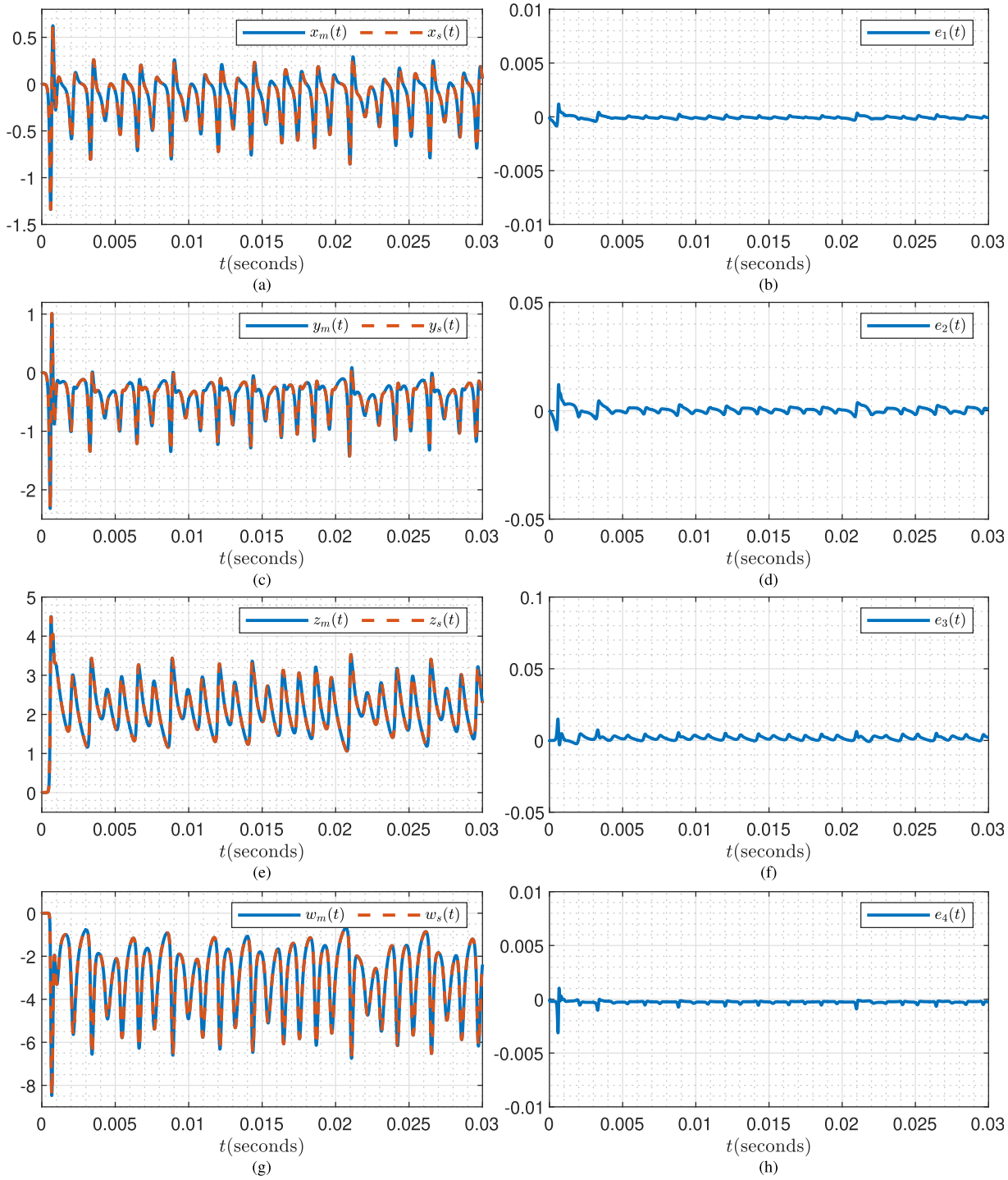

FIGURE 10. Performance of the synchronization. The states and errors are in volts.

that high gains do not prevent application since these gains can be decreased by amplitude scaling of the hyperchaotic systems leading to lower bounds for the states, as can be seen in Section VI.

V. CHAOS-BASED SECURE COMMUNICATION

In addition to the projective synchronization case, we also consider the application of the proposed method to secure telecommunication. To have a well-posed problem, the following assumption must be imposed.

Assumption 2: It is assumed that the messages are bounded. More specifically,

$$|m_i(t)| \leq \bar{m}_i, \quad i = 1, \ldots, 4 \tag{21}$$

$\forall t \geq 0$, where m_1, m_2, m_3, and m_4 are the original messages and $\bar{m}_1$, $\bar{m}_2$, $\bar{m}_3$, and $\bar{m}_4$ are positive constants.

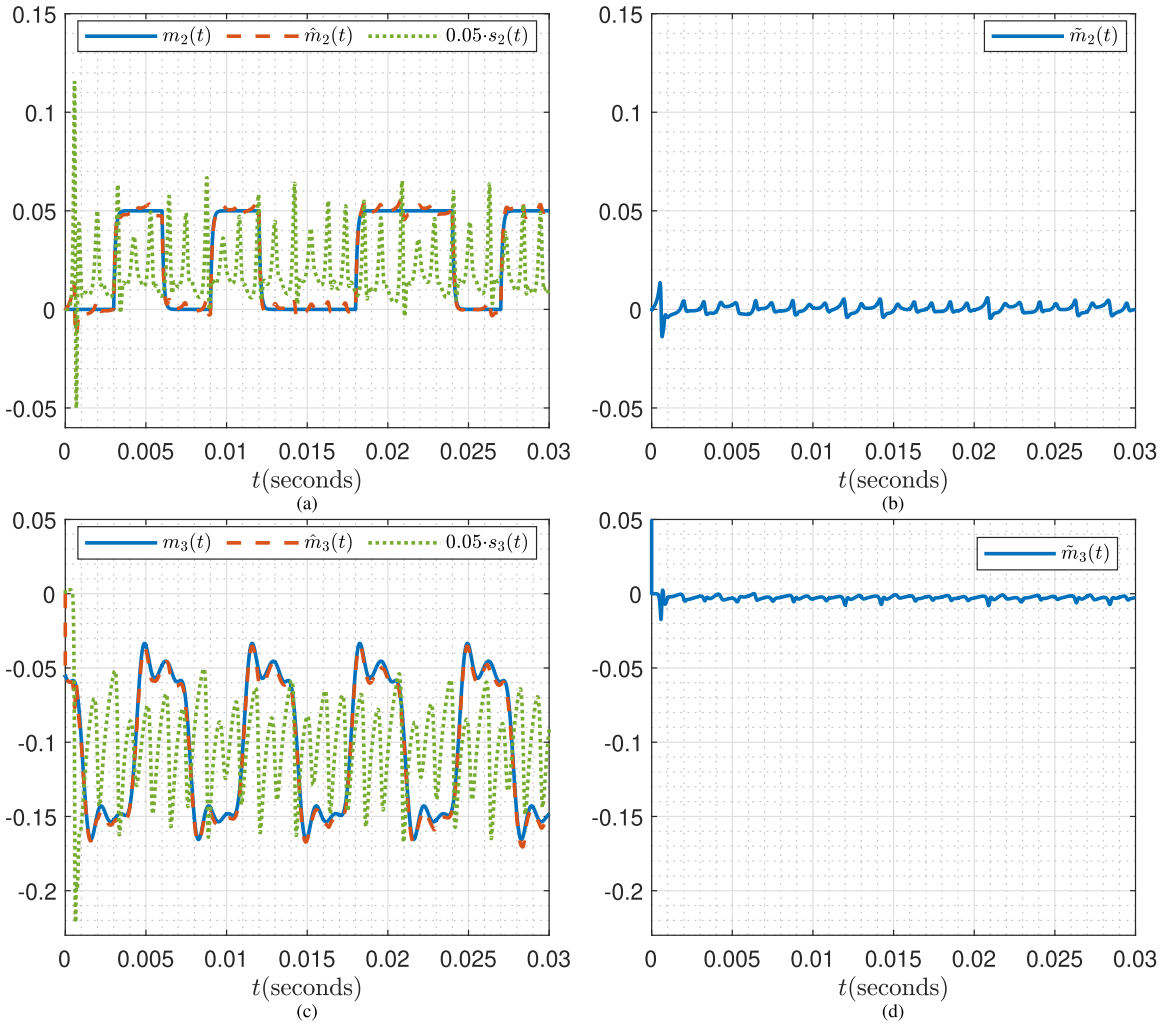

FIGURE 11. Performance of the secure communication. All signals are in volts.

Further, motivated by [38], it can be defined

$$\begin{aligned}\hat{m}_1 &= \delta[x_m + m_1] - x_s\\ \hat{m}_2 &= \delta[y_m + m_2] - y_s\\ \hat{m}_3 &= \delta[z_m + m_3] - z_s\\ \hat{m}_4 &= \delta[w_m + m_4] - w_s\end{aligned} \tag{22}$$

where $\hat{m}_1$, $\hat{m}_2$, $\hat{m}_3$, and $\hat{m}_4$ are the decoded messages.

On the other hand, by using (22) and defining $\tilde{m}_i = \hat{m}_i - \delta m_i, i = 1, \ldots, 4$, where $\tilde{m}_1$, $\tilde{m}_2$, $\tilde{m}_3$, and $\tilde{m}_4$ are the message errors, it can be concluded that

$$\tilde{m}_i = -e_i, \quad i = 1, \ldots, 4 \tag{23}$$

Remark 7: It is worth noticing that the quality of the message reconstruction is the same as the synchronization, as shown in (23). Furthermore, the boundedness of the message error is assured when the synchronization error is bounded.

VI. SIMULATIONS

Simulations were performed using Matlab/Simulink 2020b on a Windows 10 platform, with AMD Ryzen 7 1700 processor. All the scripts to reproduce the results of this paper are available with the corresponding author under request. In all simulations, it was considered that $\delta = 1$.

A. IMPLEMENTATION EXAMPLE

For implementation purposes, we consider $a = 10$, $b = 47$, $c = 1$, $d = 1$, and $k = 2$. It was also necessary to scale both the frequency and amplitude of the hyperchaotic systems (1)- (2) to decrease the transient and hold the operating voltage of the devices. The system amplitude was then decreased up to 20 times, and the system rate was increased by a factor of 1000. Hence, the scaled systems were rewritten in a condensed form as

$$\begin{cases}\dot{X} = 10^3[10(Y - X) - X + I_* u_1] + h_1\\ \dot{Y} = 10^3[47X - 20XZ - Y] + h_2\\ \dot{Z} = 10^3[20XY - Z] + h_3\\ \dot{W} = 10^3[20XZ - 2W + I_* u_4] + h_4\end{cases} \tag{24}$$

where $I_* = \{0, 1\}$, u_1 and u_4 are defined as in (7) being $\psi_1 = \psi_3 = 100$ and $\psi_2 = 10000$. Figure 1 shows the

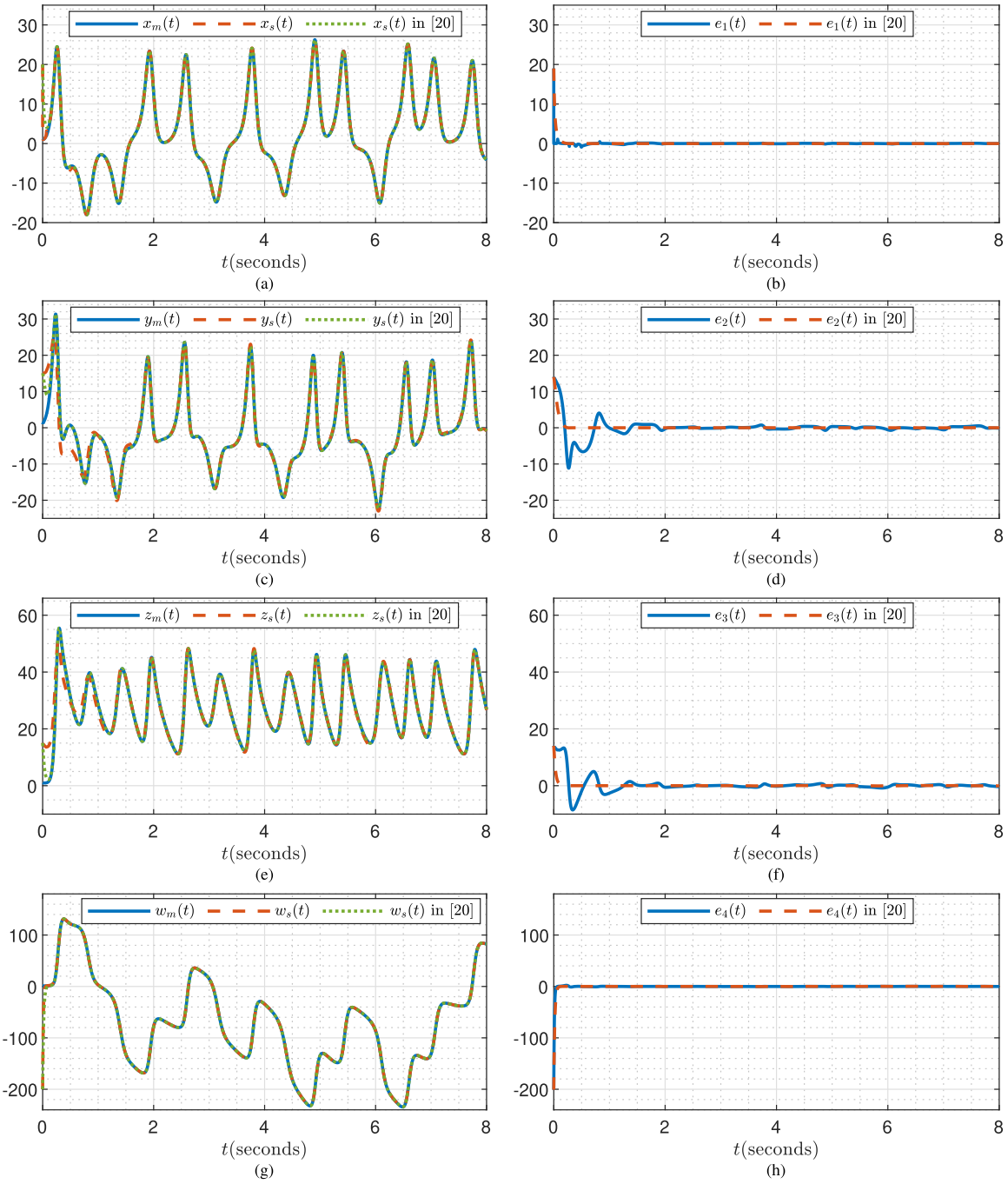

FIGURE 12. **Comparison between the proposed method and that in [20].**

circuit diagram designed by using Simscape/Simulink being their blocks detailed in Figures 2 - 9.

For the sake of conciseness, (24) was considered as being the transmitter when $I_* = 0$ (X, Y, Z, and W must be substituted by X_m, Y_m, Z_m, and W_m) and the receiver when $I_* = 1$ (in which case X, Y, Z, and W must be substituted by X_s, Y_s, Z_s, and W_s).

The encrypted signals are defined as $s_2 = m_2 + Y_m$, $s_3 = m_3 + Z_m$ and the decrypted signals as $\hat{m}_2 = s_2 - Y_s$, $\hat{m}_3 = s_3 - Z_s$. This definition was adopted to use the same circuital structure for simple encryption and decryption. The considered messages were m_2 as being a sequence of bits and $m_3 = a_0 + 0.5 \cdot \sum_{i=1}^{8}[a_i \cdot \cos(i \cdot w \cdot t) + b_i \cdot \sin(i \cdot w \cdot t)]$, where $w = 941.7$, $a_0 = -0.1009055$, $a_1 = 0.09614$, $b_1 = -0.08111$, $a_2 = -0.002126$, $b_2 = -0.002561$, $a_3 = 0.01418$, $b_3 = 0.03685$, $a_4 = 0.0004152$, $b_4 = -0.002264$, $a_5 = -0.01999$, $b_5 = -0.0121$, $a_6 = 7.883 \cdot 10^{-5}$, $b_6 = -0.0008134$, $a_7 = 0.002927$, $b_7 = -0.0009047$, $a_8 = -3.586 \cdot 10^{-5}$, and $b_8 = -0.0008205$.

In all simulations, analog multipliers AD633JNZ and operational amplifiers OPA228 are used. Nominal voltage limits, slew rate, bandwidth, input impedance, output impedance, offset voltage, and polarization current from their datasheets were also considered. Further, all capacitors and resistors used here were non-ideal with a tolerance of 0.1% to better reproduce a more realistic scenario.

Figure 10 depicts a typical performance of the synchronization using electronic circuits. The synchronization errors are small even when underactuated control and unmatched perturbations resulting from the non-ideal behavior of the devices are considered. Based on the simulations, we can conclude that the proposed method is easily implementable by analog electronics, and has good performance, as far as the synchronization error is considered.

Figure 11 shows the performance of the encryption of two message signals using the proposed synchronization method. As expected from theoretical analysis, the recovered signals converge over time close to the original ones, even in the presence of internal or external perturbations, which are due to the usage of non-ideal devices in a realistic scenario in our simulations.

B. COMPARISON WITH [20]

To better show the performance of the proposed scheme, we have compared our synchronization performance with that in [20] in the presence of disturbances. In [20], a novel synchronizer for hyperchaotic Lorenz system was introduced. Although finite-time convergence was accomplished, neither external disturbances in the stability analysis nor a simple underactuated control were considered.

The parameters used in our simulation were $a = 20$, $b = 32$, $c = 3$, $d = 1$, $k = -1$, $\psi_1 = \psi_3 = 100$, and $\psi_2 = 10000$. The initial conditions for the master and slave systems in both cases were $x_m(0) = 1$, $y_m(0) = 1$, $z_m(0) = 1$, $w_m(0) = 1$, $x_s(0) = 20$, $y_s(0) = 15$, $z_s(0) = 15$, and $w_s(0) = -200$.

Also, an unmatched disturbance was introduced to check the robustness of the proposed approach when it is compared with that in [20]. The used disturbance was defined as

$$\begin{aligned} h_1 &= 0.3 \cdot \exp(5 \cdot 10^{-5} \cdot x_s^2) \\ h_2 &= 0.2 \cdot \exp(10^{-5} \cdot y_s^2) \\ h_3 &= 3sin(3t) + cos(20t) \\ h_4 &= 5sin(10t) + 10cos(t) \end{aligned} \tag{25}$$

Three systems were simulated: the master (1), slave (2), using an underactuated control, and the slave system in [20], in which a full-actuated control is employed. From simulations shown in Figure 12, it can be seen that the performance of the proposed scheme is similar to that in [20]. However, the proposed approach is simpler than that in [20] since the proposed control is only used in the x_s and w_s channels.

VII. CONCLUSION

An underactuated scheme for projective synchronization of hyperchaotic systems based on Lyapunov theory has been proposed in this work. The main advantages of the proposed synchronization method are its simplicity, low cost of implementation, and its ability to tackle unmatched disturbances. It has been further employed in chaos-based secure communication to depict the performance of a typical application. With the use of electronic circuits, the ease of implementation has been shown as well. It should be noted that the decoded signal is close to the original, as expected, even in the presence of unmatched disturbances and underactuated control.

Potential drawbacks of the work must mention the need to use two control signals instead of just one. This is due to the topology of the considered hyperchaotic systems.

Future works will include the underactuated synchronization of hyperchaotic systems of high dimension by using online approximators such as neural networks and fuzzy systems.

REFERENCES

[1] S. H. Strogatz, *Nonlinear Dynamics and Chaos With Student Solutions Manual: With Applications to Physics, Biology, Chemistry, and Engineering*. Boca Raton, FL, USA: CRC Press, 2018, ch. 9, sec. 9.3.
[2] T. Kapitaniak and L. O. Chua, "Hyperchaotic attractors of unidirectionally-coupled Chua's circuits," *Int. J. Bifurcat. Chaos*, vol. 4, no. 2, pp. 477–482, Apr. 1994.
[3] E. N. Lorenz, "Deterministic nonperiodic flow," *J. Atmos. Sci.*, vol. 20, no. 2, pp. 130–141, Mar. 1963.
[4] O. E. Rössler, "An equation for continuous chaos," *Phys. Lett. A*, vol. 57, no. 5, pp. 397–398, Jul. 1976.
[5] G. Chen and T. Ueta, "Yet another chaotic attractor," *Int. J. Bifurcation Chaos*, vol. 9, no. 7, pp. 1465–1466, 1999.
[6] J. C. Sprott, "Simple chaotic systems and circuits," *Amer. J. Phys.*, vol. 68, no. 8, pp. 758–763, Jul. 2000.
[7] J. Lü and G. Chen, "A new chaotic attractor coined," *Int. J. Bifurcation Chaos*, vol. 12, no. 3, pp. 659–661, 2002.
[8] Z. Wang, C. Volos, S. T. Kingni, A. T. Azar, and V.-T. Pham, "Four-wing attractors in a novel chaotic system with hyperbolic sine nonlinearity," *Optik*, vol. 131, pp. 1071–1078, Feb. 2017.
[9] S. Mobayen, S. T. Kingni, V.-T. Pham, F. Nazarimehr, and S. Jafari, "Analysis, synchronisation and circuit design of a new highly nonlinear chaotic system," *Int. J. Syst. Sci.*, vol. 49, no. 3, pp. 617–630, Feb. 2018.
[10] S. Vaidyanathan, O. A. Abba, G. Betchewe, and M. Alidou, "A new three-dimensional chaotic system: Its adaptive control and circuit design," *Int. J. Autom. Control*, vol. 13, no. 1, pp. 101–121, 2019.
[11] C. Nwachioma, J. H. Pérez-Cruz, A. Jimenez, M. Ezuma, and R. Rivera-Blas, "A new chaotic oscillator—Properties, analog implementation, and secure communication application," *IEEE Access*, vol. 7, pp. 7510–7521, 2019.
[12] J. C. Sprott, *Elegant Chaos: Algebraically Simple Chaotic Flows*. Singapore: World Scientific, 2010, ch. 6, sec. 6.7, p. 152.
[13] O. E. Rössler, "An equation for hyperchaos," *Phys. Lett. A*, vol. 71, nos. 2–3, pp. 155–157, Apr. 1979.
[14] C. Li, J. C. Sprott, W. Thio, and H. Zhu, "A new piecewise linear hyperchaotic circuit," *IEEE Trans. Circuits Syst. II, Exp. Briefs*, vol. 61, no. 12, pp. 977–981, Dec. 2014.
[15] Y. Li, W. K. S. Tang, and G. Chen, "Generating hyperchaos via state feedback control," *Int. J. Bifurcation Chaos*, vol. 15, no. 10, pp. 3367–3375, 2005.
[16] Q. Jia, "Hyperchaos generated from the Lorenz chaotic system and its control," *Phys. Lett. A*, vol. 366, no. 3, pp. 217–222, Jun. 2007.
[17] K. Rajagopal, S. Vaidyanathan, A. Karthikeyan, and A. Srinivasan, "Complex novel 4D memristor hyperchaotic system and its synchronization using adaptive sliding mode control," *Alexandria Eng. J.*, vol. 57, no. 2, pp. 683–694, Jun. 2018.
[18] J. P. Singh and B. K. Roy, "Hidden attractors in a new complex generalised Lorenz hyperchaotic system, its synchronisation using adaptive contraction theory, circuit validation and application," *Nonlinear Dyn.*, vol. 92, no. 2, pp. 373–394, Jan. 2018.

[19] R. Wang, M. Li, Z. Gao, and H. Sun, "A new memristor-based 5D chaotic system and circuit implementation," *Complexity*, vol. 2018, pp. 1–12, Dec. 2018.
[20] C. Zhou, C. Yang, D. Xu, and C.-Y. Chen, "Dynamic analysis and finite-time synchronization of a new hyperchaotic system with coexisting attractors," *IEEE Access*, vol. 7, pp. 52896–52902, 2019.
[21] W. Yu, J. Wang, J. Wang, H. Zhu, M. Li, Y. Li, and D. Jiang, "Design of a new seven-dimensional hyperchaotic circuit and its application in secure communication," *IEEE Access*, vol. 7, pp. 125586–125608, 2019.
[22] P. Li, J. Du, S. Li, and Y. Zheng, "Modulus synchronization of a novel hyperchaotic real system and its corresponding complex system," *IEEE Access*, vol. 7, pp. 109577–109584, 2019.
[23] X. Wang, S. Vaidyanathan, C. Volos, V.-T. Pham, and T. Kapitaniak, "Dynamics, circuit realization, control and synchronization of a hyper-chaotic hyperjerk system with coexisting attractors," *Nonlinear Dyn.*, vol. 89, no. 3, pp. 1673–1687, May 2017.
[24] I. Admad, B. Srisuchinwong, and W. San-Um, "On the first hyperchaotic hyperjerk system with no equilibria: A simple circuit for hidden attractors," *IEEE Access*, vol. 6, pp. 35449–35456, 2018.
[25] B. A. Mezatio, M. T. Motchongom, B. R. W. Tekam, R. Kengne, R. Tchitnga, and A. Fomethe, "A novel memristive 6D hyperchaotic autonomous system with hidden extreme multistability," *Chaos, Solitons Fractals*, vol. 120, pp. 100–115, Mar. 2019.
[26] Y. Feng, Z. Wei, U. E. Kocamaz, A. Akgül, and I. Moroz, "Synchronization and electronic circuit application of hidden hyperchaos in a four-dimensional self-exciting homopolar disc dynamo without equilibria," *Complexity*, vol. 2017, pp. 1–11, May 2017.
[27] J. A. R. Vargas, W. Pedrycz, and E. M. Hemerly, "Improved learning algorithm for two-layer neural networks for identification of nonlinear systems," *Neurocomputing*, vol. 329, no. 15, pp. 86–96, Feb. 2019.
[28] K. H. M. Gularte, J. J. M. Chávez, J. A. R. Vargas, and S. C. A. Alfaro, "An adaptive neural identifier with applications to financial and welding systems," *Int. J. Control, Autom. Syst.*, vol. 19, no. 5, pp. 1976–1987, May 2021.
[29] E. Grzeidak, J. A. R. Vargas, and S. C. A. Alfaro, "ELM with guaranteed performance for online approximation of dynamical systems," *Nonlinear Dyn.*, vol. 91, no. 3, pp. 1587–1603, Feb. 2018.
[30] Y. Zhao, X. Li, and P. Duan, "Observer-based sliding mode control for synchronization of delayed chaotic neural networks with unknown disturbance," *Neural Netw.*, vol. 117, pp. 268–273, Sep. 2019.
[31] J. A. R. Vargas, K. H. M. Gularte, and E. M. Hemerly, "Adaptive observer design based on scaling and neural networks," *IEEE Latin Amer. Trans.*, vol. 11, no. 4, pp. 989–994, Jun. 2013.
[32] A. Yousefpour, H. Jahanshahi, J. M. Munoz-Pacheco, S. Bekiros, and Z. Wei, "A fractional-order hyper-chaotic economic system with transient chaos," *Chaos, Solitons Fractals*, vol. 130, Jan. 2020, Art. no. 109400.
[33] H. Wang, C. Weng, Z. Song, and J. Cai, "Research on the law of spatial fractional calculus diffusion equation in the evolution of chaotic economic system," *Chaos, Solitons Fractals*, vol. 131, Feb. 2020, Art. no. 109462.
[34] G. Bestard, R. Sampaio, J. Vargas, and S. Alfaro, "Sensor fusion to estimate the depth and width of the weld bead in real time in GMAW processes," *Sensors*, vol. 18, no. 4, p. 962, Mar. 2018.
[35] L. Zhiyong, Z. Qiang, L. Yan, Y. Xiaocheng, and T. S. Srivatsan, "An analysis of gas metal arc welding using the Lyapunov exponent," *Mater. Manuf. Processes*, vol. 28, no. 2, pp. 213–219, Feb. 2013.
[36] J. Wang, W. Yu, J. Wang, Y. Zhao, J. Zhang, and D. Jiang, "A new six-dimensional hyperchaotic system and its secure communication circuit implementation," *Int. J. Circuit Theory Appl.*, vol. 47, no. 5, pp. 702–717, Mar. 2019.
[37] B. Naderi and H. Kheiri, "Exponential synchronization of chaotic system and application in secure communication," *Optik*, vol. 127, no. 5, pp. 2407–2412, Mar. 2016.
[38] B. Jovic, *Synchronization Techniques for Chaotic Communication Systems*. Berlin, Germany: Springer-Verlag, 2011.
[39] N. Smaoui, A. Karouma, and M. Zribi, "Secure communications based on the synchronization of the hyperchaotic Chen and the unified chaotic systems," *Commun. Nonlinear Sci. Numer. Simul.*, vol. 16, no. 8, pp. 3279–3293, Aug. 2011.
[40] P. Liu, R. Xi, P. Ren, J. Hou, and X. Li, "Analysis and implementation of a new switching memristor scroll hyperchaotic system and application in secure communication," *Complexity*, vol. 2018, pp. 1–15, Jul. 2018.
[41] W. Yan and Q. Ding, "A new matrix projective synchronization and its application in secure communication," *IEEE Access*, vol. 7, pp. 112977–112984, 2019.
[42] H.-P. Ren, M. S. Baptista, and C. Grebogi, "Wireless communication with chaos," *Phys. Rev. Lett.*, vol. 110, no. 18, Apr. 2013, Art. no. 184101.
[43] F. Yu, Q. Wan, J. Jin, L. Li, B. He, L. Liu, S. Qian, Y. Huang, S. Cai, Y. Song, and Q. Tang, "Design and FPGA implementation of a pseudo-random number generator based on a four-wing memristive hyperchaotic system and Bernoulli map," *IEEE Access*, vol. 7, pp. 181884–181898, 2019.
[44] Q. Liu and L. Liu, "Color image encryption algorithm based on DNA coding and double chaos system," *IEEE Access*, vol. 8, pp. 83596–83610, 2020.
[45] J. Xu, P. Li, F. Yang, and H. Yan, "High intensity image encryption scheme based on quantum logistic chaotic map and complex hyperchaotic system," *IEEE Access*, vol. 7, pp. 167904–167918, 2019.
[46] X. Wang and L. Liu, "Image encryption based on hash table scrambling and DNA substitution," *IEEE Access*, vol. 8, pp. 68533–68547, 2020.
[47] S. Zhu and C. Zhu, "Plaintext-related image encryption algorithm based on block structure and five-dimensional chaotic map," *IEEE Access*, vol. 7, pp. 147106–147118, 2019.
[48] X. Min, X. Wang, P. Zhou, S. Yu, and H. H.-C. Iu, "An optimized memristor-based hyperchaotic system with controlled hidden attractors," *IEEE Access*, vol. 7, pp. 124641–124646, 2019.
[49] F. Yu, H. Shen, L. Liu, Z. Zhang, Y. Huang, B. He, S. Cai, Y. Song, B. Yin, S. Du, and Q. Xu, "CCII and FPGA realization: A multistable modified fourth-order autonomous Chua's chaotic system with coexisting multiple attractors," *Complexity*, vol. 2020, pp. 1–17, Mar. 2020.
[50] B. Bao, Q. Yang, L. Zhu, H. Bao, Q. Xu, Y. Yu, and M. Chen, "Chaotic bursting dynamics and coexisting multistable firing patterns in 3D autonomous Morris–Lecar model and microcontroller-based validations," *Int. J. Bifurcation Chaos*, vol. 29, no. 10, Sep. 2019, Art. no. 1950134.
[51] H. Takhi, K. Kemih, L. Moysis, and C. Volos, "Passivity based control and synchronization of perturbed uncertain chaotic systems and their microcontroller implementation," *Int. J. Dyn. Control*, vol. 8, pp. 973–990, Mar. 2020.
[52] S. He, K. Sun, H. Wang, X. Mei, and Y. Sun, "Generalized synchronization of fractional-order hyperchaotic systems and its DSP implementation," *Nonlinear Dyn.*, vol. 92, no. 1, pp. 85–96, Apr. 2018.
[53] X. Wu, Z. Fu, and J. Kurths, "A secure communication scheme based generalized function projective synchronization of a new 5D hyperchaotic system," *Phys. Scripta*, vol. 90, no. 4, Mar. 2015, Art. no. 045210.
[54] G. Pérez and H. A. Cerdeira, "Extracting messages masked by chaos," *Phys. Rev. Lett.*, vol. 74, no. 11, p. 1970, Mar. 1995.
[55] L. Cao, "A four-dimensional hyperchaotic finance system and its control problems," *J. Control Sci. Eng.*, vol. 2018, pp. 1–12, Feb. 2018.
[56] L. M. Pecora and T. L. Carroll, "Synchronization in chaotic systems," *Phys. Rev. Lett.*, vol. 64, no. 8, pp. 821–824, Feb. 1990.
[57] D. Liu, S. Zhu, and K. Sun, "Global anti-synchronization of complex-valued memristive neural networks with time delays," *IEEE Trans. Cybern.*, vol. 49, no. 5, pp. 1735–1747, May 2019.
[58] G. Al-Mahbashi and M. S. M. Noorani, "Finite-time lag synchronization of uncertain complex dynamical networks with disturbances via sliding mode control," *IEEE Access*, vol. 7, pp. 7082–7092, 2019.
[59] J. Yan and C. Li, "Generalized projective synchronization of a unified chaotic system," *Chaos, Solitons Fractals*, vol. 26, no. 4, pp. 1119–1124, Nov. 2005.
[60] R. Mainieri and J. Rehacek, "Projective synchronization in three-dimensional chaotic systems," *Phys. Rev. Lett.*, vol. 82, no. 15, p. 3042, Apr. 1999.
[61] G.-H. Li, "Modified projective synchronization of chaotic system," *Chaos, Solitons Fractals*, vol. 32, no. 5, pp. 1786–1790, Jun. 2007.
[62] S. Chen and J. Cao, "Projective synchronization of neural networks with mixed time-varying delays and parameter mismatch," *Nonlinear Dyn.*, vol. 67, no. 2, pp. 1397–1406, Jan. 2012.
[63] R. Kumar, S. Sarkar, S. Das, and J. Cao, "Projective synchronization of delayed neural networks with mismatched parameters and impulsive effects," *IEEE Trans. Neural Netw. Learn. Syst.*, vol. 31, no. 4, pp. 1211–1221, Apr. 2020.
[64] H. Du, Q. Zeng, and C. Wang, "Function projective synchronization of different chaotic systems with uncertain parameters," *Phys. Lett. A*, vol. 372, no. 33, pp. 5402–5410, Aug. 2008.
[65] M. Krstic, P. Kokotovic, and I. Kanellakopoulos, *Nonlinear and Adaptive Control Design*. Hoboken, NJ, USA: Wiley, 1995.
[66] A. Zarei and S. Tavakoli, "Synchronization of quadratic chaotic systems based on simultaneous estimation of nonlinear dynamics," *J. Comput. Nonlinear Dyn.*, vol. 13, no. 8, Aug. 2018, Art. no. 081001.

[67] L. P. N. Nguenjou, G. H. Kom, J. R. M. Pone, J. Kengne, and A. B. Tiedeu, "A window of multistability in Genesio–Tesi chaotic system, synchronization and application for securing information," *AEU, Int. J. Electron. Commun.*, vol. 99, pp. 201–214, Feb. 2019.
[68] S. Singh, "Single input sliding mode control for hyperchaotic Lü system with parameter uncertainty," *Int. J. Dyn. Control*, vol. 4, no. 4, pp. 504–514, Dec. 2016.
[69] J. A. R. Vargas, E. Grzeidak, K. H. M. Gularte, and S. C. A. Alfaro, "An adaptive scheme for chaotic synchronization in the presence of uncertain parameter and disturbances," *Neurocomputing*, vol. 174, pp. 1038–1048, Jan. 2016.
[70] J. A. R. Vargas, E. Grzeidak, and E. M. Hemerly, "Robust adaptive synchronization of a hyperchaotic finance system," *Nonlinear Dyn.*, vol. 80, nos. 1–2, pp. 239–248, Apr. 2015.
[71] J. Moreno-Valenzuela and C. Aguilar-Avelar, *Motion Control of Underactuated Mechanical Systems*. Cham, Switzerland: Springer, 2018.
[72] J. Moreno–Valenzuela, J. Montoya–Cháirez, and V. Santibáñez, "Robust trajectory tracking control of an underactuated control moment gyroscope via neural network–based feedback linearization," *Neurocomputing*, vol. 403, pp. 314–324, Aug. 2020.
[73] I. Fantoni, R. Lozano, and S. C. Sinha, "Non-linear control for underactuated mechanical systems," *Appl. Mech. Rev.*, vol. 55, no. 4, pp. B67–B68, 2002.
[74] S. Rudra, R. K. Barai, and M. Maitra, *Block Backstepping Design of Nonlinear State Feedback Control Law for Underactuated Mechanical Systems*. Singapore: Springer, 2017, p. 1.
[75] B. Monga and J. Moehlis, "Supervised learning algorithms for controlling underactuated dynamical systems," *Phys. D, Nonlinear Phenomena*, vol. 412, Nov. 2020, Art. no. 132621.
[76] A. Sabaghian and S. Balochian, "Parameter estimation and synchronization of hyper chaotic Lu system with disturbance input and uncertainty using two under-actuated control signals," *Trans. Inst. Meas. Control*, vol. 41, no. 6, pp. 1729–1739, Apr. 2019.
[77] A. Loría, "A linear time-varying controller for synchronization of Lü chaotic systems with one input," *IEEE Trans. Circuits Syst. II, Exp. Briefs*, vol. 56, no. 8, pp. 674–678, Aug. 2009.
[78] P. Ioannou and J. Sun, *Robust Adaptive Control*. Upper Saddle River, NJ, USA: Prentice-Hall, 1995.
[79] E. Lavretsky and K. A. Wise, *Robust and Adaptive Control: With Aerospace Applications*. London, U.K.: Springer-Verlag, 2013, p. 248.
[80] M. K. Shukla and B. B. Sharma, "Backstepping based stabilization and synchronization of a class of fractional order chaotic systems," *Chaos, Solitons Fractals*, vol. 102, pp. 274–284, Sep. 2017.
[81] S. Ha, H. Liu, S. Li, and A. Liu, "Backstepping-based adaptive fuzzy synchronization control for a class of fractional-order chaotic systems with input saturation," *Int. J. Fuzzy Syst.*, vol. 21, no. 5, pp. 1571–1584, Jul. 2019.
[82] Q. Yao, "Synchronization of second-order chaotic systems with uncertainties and disturbances using fixed-time adaptive sliding mode control," *Chaos, Solitons Fractals*, vol. 142, Jan. 2021, Art. no. 110372.
[83] V. R. F. Signing, J. Kengne, and L. K. Kana, "Dynamic analysis and multistability of a novel four-wing chaotic system with smooth piecewise quadratic nonlinearity," *Chaos, Solitons Fractals*, vol. 113, pp. 263–274, Aug. 2018.
[84] S. Vaidyanathan, A. Sambas, and M. Mamat, "A new chaotic system with axe-shaped equilibrium, its circuit implementation and adaptive synchronization," *Arch. Control Sci.*, vol. 28, no. 3, pp. 443–462, 2018.

KEVIN HERMAN MURARO GULARTE received the B.Sc. degree in mechatronics engineering and the M.Sc. degree in mechatronic systems from the University of Brasilia, in 2013 and 2018, respectively, where he is currently pursuing the Dr.Sc. degree in electronic and automation systems engineering. His research interests include systems synchronization, chaotic systems, adaptive control, neural networks, Lyapunov theory, and systems identification.

LUCAS MARTINS ALVES is currently pursuing the B.Sc. degree in electrical engineering with the University of Brasilia (UnB). His current research interests include neural networks, electronics, and synchronization of chaotic systems.

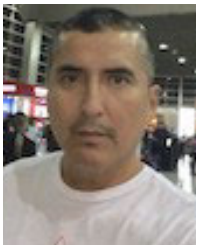

JOSÉ ALFREDO RUIZ VARGAS received the Dr.Sc. degree in electronics and computer engineering from the Aeronautics Institute of Technology, São Paulo, Brazil, in 2003. From 2016 to 2017, he was a Visiting Professor at the University of Alberta, Edmonton, AB, Canada. He is a Professor of control systems with the Department of Electrical Engineering, University of Brasilia. His current research interests include chaotic systems, nonlinear control, adaptive control, and online machine learning.

SADEK CRISÓSTOMO ABSI ALFARO received the B.Sc. degree in mechanical engineering from the Federal University of Rio Grande do Sul (UFRGS), in 1979, the M.Sc. degree in metallurgical engineering from the Federal University of Minas Gerais (UFMG), in 1983, and the Ph.D. and postdoctoral degrees in welding engineering from the School of Industrial and Manufacturing Science, Cranfield Institute, U.K., in 1989 and 1990, respectively. Since 1983, he has been a Lecturer with the University of Brasilia, where he held the position of Full Professor at the Department of Mechanical/Mechatronic Engineering, from 2003 to 2017, developing activities on undergraduate and postgraduate studies and research activities and coordinated research and development projects. Currently, he is a Senior Researcher at the University of Brasilia.

GUILHERME CARIBE DE CARVALHO received the B.Sc. degree in aeronautical and mechanical engineering from the Aeronautics Institute of Technology, São Paulo, Brazil, in 1989, the M.Sc. degree in mechanical engineering from the University of Brasilia, in 1993, and the Ph.D. degree in welding technology from Cranfield University, U.K., in 1997. He was admitted as a Lecturer at the University of Brasilia, in 1998. Currently, he holds the position of Associate Professor at the Mechanical Engineering Department, University of Brasilia. Since then, he has developed lecturing and research activities on industrial robotics, robotic welding, welding process instrumentation, industrial automation, and more recently, wire and arc additive manufacturing.

JESUS FRANKLIN ANDRADE ROMERO received the B.Sc. degree in electrical engineering from the Higher University of San Andrés, Bolivia, in 1992, and the M.Sc. and Dr.Sc. degrees in electrical engineering from the Aeronautics Institute of Technology, São Paulo, Brazil, in 1997 and 2002, respectively. He joined the Federal University of ABC, São Paulo, in 2006, where he is currently an Associate Professor with the Center for Engineering, Modeling, and Applied Social Sciences. His research interests include control and supervisory systems, digital signal processing, and nonlinear systems.